A Hybrid Polymer Gel and Its Static Nonergodicity

Yue Zhao,[1] *Chi Wu**[1,2]

[1] The Open Laboratory of Bond Selective Chemistry, Department of Chemical Physics, University of Science and Technology of China, Hefei, Anhui, China
[2] Department of Chemistry, The Chinese University of Hong Kong, Shatin, N.T., Hong Kong
* The Hong Kong address should be used for correspondence.

Summary: We used a thermally reversible hybrid gel made of billions of *physically* jam-packed, swollen, thermally sensitive poly(*N*-isopropyl-acrylamide) *chemical* microgels. Laser light scattering study on a series of such hybrid gels formed at different gelling rates and temperatures revealed that the position-dependence of the scattering speckle pattern (static nonergodicity) came from large voids formed during the sol-gel transition. With proper preparation, such nonergodicity is completely removed, indicating that the static nonergodicity generally observed in a gel is not intrinsic, but comes from clustering "island" structures formed during the gelation process.

Introduction

A gel is generally considered to be a three-dimensional polymer network swollen by a large amount of solvent. Polymer chains in chemical gels are crosslinked by covalent bonds. A chemical gel is normally formed by a copolymerization of monomers with a crosslinking agent.[1-4] In contrast, the formation of a physical gel usually starts with a polymer solution. In physical gels, polymer chains are interconnected via physical interactions (e.g., hydrogen bonding, electrostatic interaction, and coordination) and the gelation is often induced by an alternation of physical conditions, such as temperature and ionic strength.[5] It has been well known that in the formation of chemical gels, short linear chains are first formed, then large branched clusters, and finally a network in which the interconnected clusters are looked like "islands" in a three-dimensional solvent "sea."[6-10] Such an inhomogeneous clustering structure should be absent when long polymer chains uniformly distributed in a solution are randomly associated to form a physical gel.

Recently, it has been shown that there also exists a scattering speckle pattern when an aqueous mixture of poly(vinyl alcohol) and Congo red is gelled at 43 °C or below.[5] The question is whether this static nonergodicity is intrinsic for all thermally reversible physical gels or only for this particular one. In order to have a better understanding of

 DOI: 10.1002/masy.200450304

the gelation of physical gels, we have developed a novel hydrogel made of billions of thermally sensitive poly(*N*-isopropylacrylamide) (PNIPAM) microgels that jam-pack when they swell at ~25 °C or lower temperatures. Inside each microgel, the polymer chains are *chemically* crosslinked, but the interaction between the microgels is purely *physical*. This is why it is named "hybrid". It resembles a glass in which spherical swollen soft microgels replaces small atoms or molecules. It is actually formed via a volume concentration-induced gelation.

There are several advantages of using this hybrid gel as a model system to study the sol-gel transition and structures of physical gels. Advantages include: the structural inhomogeneity from chemical crosslinking is limited to length scales much smaller than the wavelength of our laser light, so that individual swollen microgels are transparent; the microgel building blocks are narrowly distributed and well characterized; and gelation is completely thermally reversible without any hysteresis. Using a combination of static and dynamic laser light scattering, we studied a series of such hybrid gels formed at different gelling rates and temperatures. It has been found that the observed scattering speckle pattern in thermally reversible physical gels is not intrinsic, but strongly depends on whether large voids were formed during gelation.

Experimental

Narrowly distributed spherical poly(*N*-isopropylacrylamide) (PNIPAM) microgels were prepared by emulsion polymerization of *N*-isopropylacrylamide in the presence of *N,N'*-methylenebis-(acrylamide) as crosslinker and anionic surfactant (sodium dodecyl sulfate, SDS) as dispersant. The unreacted monomers and SDS were removed by a three successive centrifugation-decantation-redispersion cycles in deionized water. The zeta potential of the resultant dispersion was close to zero. The synthesis has been detailed before [11,12]. A commercial LLS spectrometer (ALV/SP-125) equipped with an ALV-5000 multi-τ digital time correlator and a solid-state laser (DPSS, output power $\cong$ 400 mw at λ = 532 nm) was used in this study. The details of LLS instrumentation and theory can be found elsewhere.[13-15]

Results and Discussion

Figure 1 shows that in the gel state, the time average scattered intensity $\langle I \rangle_T$ randomly varies with the sample position. In contrast, the scattering speckle pattern disappears at

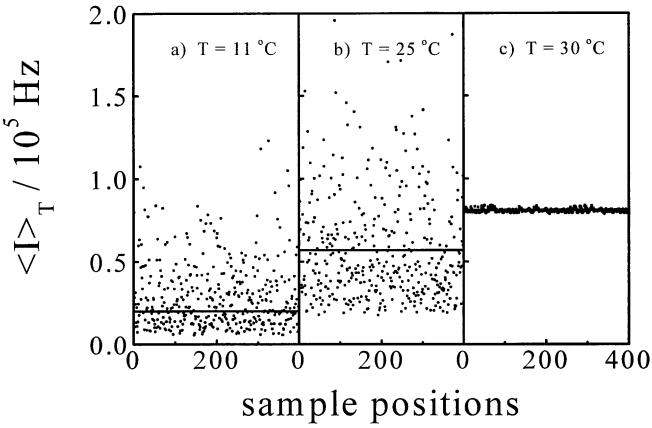

Figure 1. Sample position dependence of time-average scattered intensity $\langle I \rangle_T$ of hybrid PNIPAM gel after the microgel dispersion was quickly cooled down from 40 °C to different setting temperatures, where each solid line represents an ensemble-average intensity $\langle I \rangle_E$ defined as $(\sum_i \langle I \rangle_{T,i})/N$ with N being the total number of the sample positions measured.

30 °C because the bulk hybrid gel melts into a microgel dispersion (i.e., the sol state) due to the shrinking of individual microgels. It is worth noting that in the temperature range 15-33 °C, the microgels in a dilute dispersion can reversibly swell and shrink with a size change between ~45 nm and ~106 nm, corresponding to a 13-fold variation in volume. This is why swelling could induce the sol-gel transition. Note that $\langle I \rangle_E$ increases with the temperature, very differently from previous observations in which $\langle I \rangle_E$ decreased when a physical gel melted into individual less scattered polymer chains,[5] but similarly to a concentration induced sol-gel transition. This difference can be attributed to the fact that in this study, individual collapsed microgels are stronger scattering objects than the swollen gel network, especially when the temperature approaches its LCST.

Besides $\langle I \rangle_T$, for each chosen sample position, we also measure a normalized intensity-intensity time correlation function $S(q, \tau)$ defined as[16,17]

$$\mathbf{S(q,\tau)} = \frac{\langle \mathbf{I(q,0)I(q,\tau)} \rangle}{\langle \mathbf{I(q,0)} \rangle^2} - \mathbf{1} \qquad (1)$$

where q is the scattering vector and τ is the delay time. We found that in the gel state, the plot of "log[S(q, τ)] vs log(τ)" had a typical power-law behavior with a critical exponent close to ~0.8, higher than ~0.4 reported in [5], indicating that the hybrid gel better resembles a glass.[18] As shown in [16,17,19,20], for a nonergodic gel, $\langle I \rangle_T$ is the summation of the static component $\langle I_s \rangle_T$ and the dynamic component $\langle I_d \rangle_T$, so that

$$S(q,\tau) = \left(\frac{\langle I_d \rangle_T}{\langle I \rangle_T}\right)^2 \exp(-2Dq^2\tau) + 2\left(\frac{\langle I_d \rangle_T}{\langle I \rangle_T}\right)\left[1 - \left(\frac{\langle I_d \rangle_T}{\langle I \rangle_T}\right)\right]\exp(-Dq^2\tau) \qquad (2)$$

where D is the collective diffusion coefficient. Therefore, for a nonergodic system at a given q, one has four different scattered intensities, $\langle I \rangle_T$, $\langle I_s \rangle_T$, $\langle I_d \rangle_T$ and $\langle I \rangle_E$, but the former three are not independent. $\langle I \rangle_T$ and $\langle I_s \rangle_T$ varies with the sample position, but not $\langle I \rangle_E$ and $\langle I_d \rangle_T$ by their definitions. Only in an ergodic system is $\langle I_s \rangle_T = 0$, so that we have $\langle I \rangle_T = \langle I_d \rangle_T = \langle I \rangle_E$. Experimentally, the initial slope of "lnS(q, τ) vs τ" leads to an apparent diffusion coefficient D_A in the range of $D/2 < D_A < D$. It has been shown that D and $\langle I_d \rangle_T$ are related to D_A and $\langle I \rangle_T$ as[2,7]

$$\frac{\langle I \rangle_T}{D_A} = \frac{2\langle I \rangle_T}{D} - \frac{\langle I_d \rangle_T}{D} \qquad (3)$$

For each chosen sample position at a given q, we can measure one $\langle I \rangle_T$ from static LLS and calculate one D_A from S(q, τ) measured in dynamic LLS. Figure 2 shows that D_A decreases as $\langle I \rangle_T$ increases and approaches a constant when $\langle I \rangle_T$ is sufficiently high. The inset is a corresponding plot on the basis of eq 3. A least-squares fit of the data leads to D and $\langle I_d \rangle_T$, respectively, from its slope and intercept.

Figure 3 shows that when T < 25 °C, $\langle I \rangle_E$ increases with the temperature, but $\langle I_d \rangle_T$ remains nearly constant; while in the higher temperature range, $\langle I_d \rangle_T$ increases sharply and catches $\langle I \rangle_E$ at ~30 °C, indicating a progressive melting of the hybrid gel into individual collapsed microgels, i.e., from a nonergodic bulk gel to a completely ergodic microgel dispersion. The extrapolations of $\langle I_d \rangle_T$ in the two temperature regions leads to a temperature close to the gelation temperature (T_{gel}) observed in a flow test. Note that a high value of $\langle I \rangle_E$ was often used in the past as an indication of the inhomogeneity.

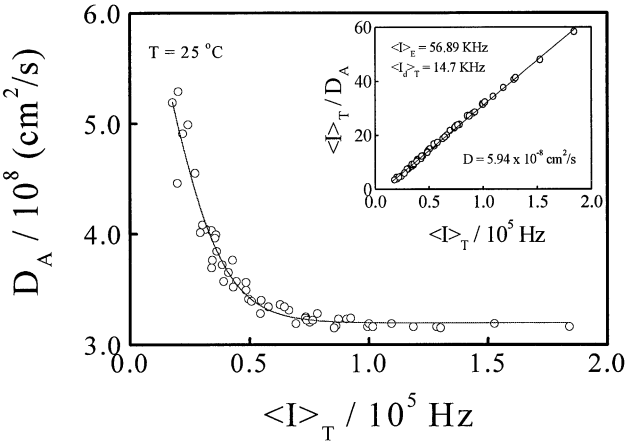

Figure 2. Time-average scattered intensity $\langle I_T \rangle$ dependence of apparent diffusion coefficient D_A of hybrid PNIPAM gel at 25 °C, where D_A was obtained from the initial slope of the intensity-intensity time correlation function. The inset shows a decomposition plot on the basis of Eq 3.

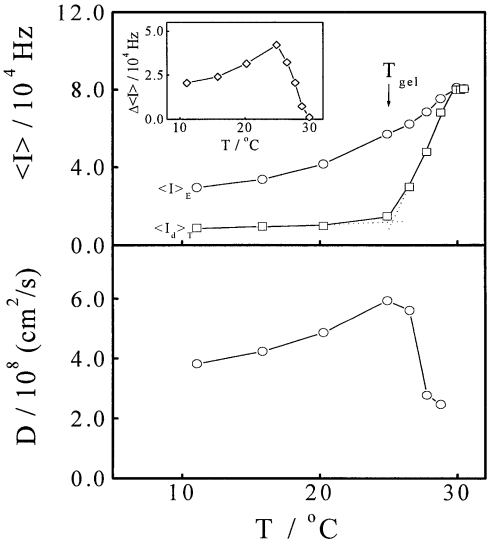

Figure 3. Temperature dependence of ensemble-average scattered intensity $\langle I \rangle_E$, time average dynamic component of scattered intensity $\langle I_d \rangle_T$ and collective diffusion coefficient D of hybrid PNIPAM gel. The arrow shows the gelation temperature T_{gel} observed by a flow test. The inset is the temperature dependence of the intensity difference (ΔI) between $\langle I \rangle_E$ and $\langle I_d \rangle_T$.

However, our result tells a different story because we know that the microgel dispersion at ~30 °C is homogeneous and ergodic even though $\langle I \rangle_E$ is higher.

Careful examination of Figure 3 reveals that *it should be the difference between* $\langle I \rangle_E$ *and* $\langle I_d \rangle_T$ *that reflects the extent of the inhomogeneity of a give system, not* $\langle I \rangle_E$ *alone*. The inset in Figure 3 shows that even before reaching the gelation threshold, the system already becomes inhomogeneous, i.e., $\Delta I > 0$. As the temperature decreases, the intensity difference ΔI reaches a maximum at T_{gel} and then decreases in the lower temperature range. This is because large voids are formed at the gelation threshold and further swelling of individual microgels squeezes the voids between the jam-packed microgels, leading to a more uniform hybrid gel. The temperature dependence of D shows a similar tendency. The jump-wise decrease in D near T_{gel} was also observed for other physical gels,[5] but not for chemical gels,[2] probably because the formation of a chemical gel is irreversible and the size of the clusters always increases during gelation. In the present case, as the temperature increases, individual microgels shrink so that non-jammed microgels diffuse rapidly. Above the melting temperature, the gel network breaks into slowly diffusing large clusters so that D decreases. It is worth noting that the value of D is close to that of individual microgels in a dilute dispersion. Since individual swollen microgels are transparent to the light used, the inhomogeneities observed in Figure 1 must come from an imperfect packing of the microgels when they were suddenly jammed together. Therefore, if we slow down the cooling process, the swollen microgels would have time to arrange themselves into a more uniform structure. Ideally, if individual collapsed microgels could be closely stacked together at a high temperature before cooling them down, we might be able to obtain a uniform hybrid gel. Figure 4 shows a schematic of how the gel structure could be influenced by the gelation condition. The different inhomogeneities shown in Figure 4 have been confirmed in terms of the scattering speckle pattern and the difference between $\langle I \rangle_E$ and $\langle I_d \rangle_T$, as shown in Figure 5. It should be stated that the hybrid gel prepared under centrifugation showed a color if is was illuminated with white light even, though it could not completely disperse the white light as a prism or a crystal. This imperfect dispersion might be attributed to the polydispersity in the microgel size and a small refractive index contrast between water and smollen microgel networks, but it clearly indicates a certain degree of ordering of the microgels inside the hybrid bulk gel.

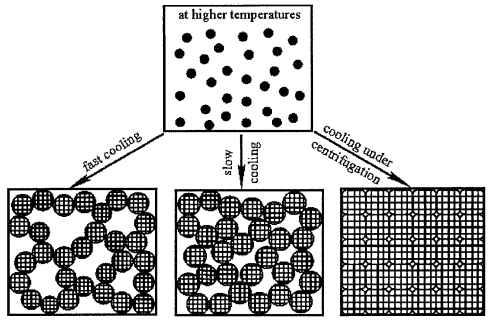

Figure 4. Schematic of the gelation condition dependence of the structure of the hybrid gel made of spherical thermally sensitive swollen PNIPAM microgels.

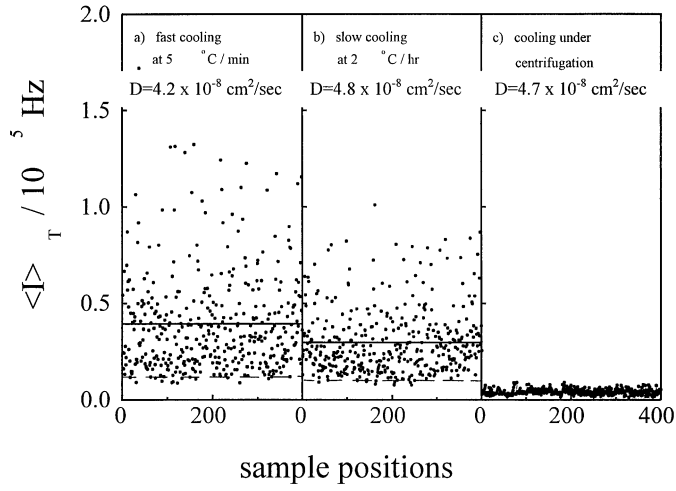

Figure 5. Sample position dependence of time-average scattered intensity $\langle I \rangle_T$ of hybrid PNIPAM gel after the microgel dispersion was cooled down from 40 °C to 15 °C under different conditions, where the solid and dashed lines represent $\langle I \rangle_E$ and $\langle I_d \rangle_T$, respectively.

Note that Figures 1c and 5c are similar. Both of them display an ergodic behavior, i.e., $\langle I \rangle_E = \langle I_d \rangle_T$. However, it is worth noting that they were obtained from two completely different states; namely, Figure 1c shows a measurement of a uniform and ergodic microgel dispersion in which individual collapsed microgels are under random Brownian motions in water, while Figure 5c is from a uniform hybrid gel. To our knowledge, this is the first observation of such a uniform and ergodic hybrid gel.

Figure 5 clearly demonstrates that the static inhomogeneity of thermally reversible physical gels is not intrinsic, but is very strongly dependent of the gelation process. It is also interesting to note that D is nearly a constant, which indicates that the voids inside the gel network are much larger than the microgels and the gel network does not affect the relaxation of individual non-jammed microgels. As expected, for a given temperature, individual non-jammed microgels with the same size relax at the same rate. How the gel network is formed can only affects the static part, i.e., $<I_d>$, but not D. This point has been overlooked in the past.

Conclusion

It is not difficult to imagine that below the gelation threshold, swollen clusters look like "islands" floating in a solvent "sea", but after gelation, the interconnected clusters become a "continent" (background) and the "sea" changes into many "lakes" (voids).[8,9,21,22] It is these large and non-uniform voids that lead to the scattering speckle pattern, and static nonergodicity. Our results suggest that this kind of static nonergodicity in both physical and chemical gels might have a similar origin. The only difference is that in chemical gels, the clusters are known to be branched polymer chains and microgels, but in physical gels, they could be formed via a non-uniform interchain association of polymer chains prior to the gelation threshold.

Acknowledgements. The financial support of the NNSF Fund (29974027), the CAS Bei Ren Project, and the Research Grants Council of the Hong Kong Special Administration Region Earmarked Grant (CUHK 4266/00P, 2160135) are gratefully acknowledged.

[1] E. Sato-Matsuo, M. Orkisz, S. T. Sun, Y. Li and T. Tanaka, *Macromolecules* **1994**, *27*, 6791 and references therein.
[2] M. Shibayama, T. Norisuye and S. Nomura, *Macromolecules* **1996**, *29*, 8746.
[3] M. Shibayama, S. Takata and T. Norisuye, *Physica A* **1998**, *249*, 245.
[4] M. Shibayama, Macromol. *Chem. Phys.* **1998**, *199*, 1.
[5] F. Ikkai and M. Shibayama, *Phys. Rev. Lett.* **1999**, *82*, 4946.
[6] M. Shibayama, M. Morimoto and S. Nomura, *Macromolecules* **1994**, *27*, 5060.
[7] M. Shibayama, Y. Fujikawa and S. Nomura, *Macromolecules* **1996**, *29*, 6535.
[8] C. Wu, J. Zuo and B. Chu, *Macromolecules* **1989**, *22*, 633.
[9] C. Wu, J. Zuo and B. Chu, *Macromolecules* **1989**, *22*, 838.
[10] C. Wu, B. Chu and G. Stell, *Makromol. Chem., Macromol. Symp.* **1989**, *45*, 75.
[11] S. Q. Zhou and B. Chu, *J. Phys. Chem. B* **1998**, *102*, 1364.

[12] C. Wu and S. Q. Zhou, *J. Polym. Sci., Polym. Phys. Ed*. **1996**, *34*, 1597.
[13] C. Wu and S. Q. Zhou, *Macromolecules* **1995**, *28*, 3375.
[14] B. Chu, *Laser Light Scattering* (Academic Press: New York, 1991), 2nd ed.
[15] B. Berne; R. Pecora, *Dynamic Light Scattering* (Plenum Press: New York, 1976).
[16] P. N. Pusey and W. van Mergen, *Physica A* **1989**, *157*, 705.
[17] J. G. H. Joosten, J. L. McCarthy and P. N. Pusey, *Macromolecules* **1991**, *24*, 6690.
[18] J. E. Martin, J. Wilcoxon and J. Odinek, *Phys. Rev. A* **1991**, *43*, 858.
[19] T. Tanaka, L. O. Hocker and G. B. Benedek, *J. Chem. Phys*. **1973**, *59,* 5151.
[20] F. Horkay. *Macromolecules* **1993**, *26*, 3375.
[21] T. Norisuye, M. Shibayama, S. Nomura, *Polymer* **1998**, *39,* 2769.
[22] T. Norisuye, M. Inoue, M. Shibayama, R. Tamaki, Y. Chujo, *Macromolecules* **2000**, *33*, 900.